International Journal of Laboratory Hematology
The Official journal of the International Society for Laboratory Hematology

CHARACTERIZATION AND AUTOMATIC SCREENING OF REACTIVE AND ABNORMAL NEOPLASTIC B LYMPHOID CELLS FROM PERIPHERAL BLOOD

Journal:	*International Journal of Laboratory Hematology*
Manuscript ID:	Draft
Manuscript Type:	Original Article
Date Submitted by the Author:	n/a
Complete List of Authors:	Alferez, Santiago; Technical University of Catalonia, Applied Mathematics III Merino, Anna; Hospital Clinic, Hemotherapy-Hemostasis Bigorra, Laura; Technical University of Catalonia, Applied Mathematics III Rodellar, Jose; Technical University of Catalonia, Applied Mathematics III
Keywords:	Lymphoma, Leukemia, Morphology, B-Cells, Blood

1. Title page

CHARACTERIZATION AND AUTOMATIC SCREENING OF REACTIVE AND ABNORMAL NEOPLASTIC B LYMPHOID CELLS FROM PERIPHERAL BLOOD

Santiago Alférez (PhD)[1], Anna Merino (MD, PhD),[2] Laura Bigorra (Clinical Pathologist),[1,2] and José Rodellar (Prof.)[1]

[1]Technical University of Catalonia, Matematica Aplicada III, Spain, and [2]Department of Hemotherapy-Hemostasis, Hospital Clinic, Barcelona, Spain

Key Words: Abnormal lymphoid cells; Blood cells; Digital image processing; Automatic cell classification; Peripheral blood; Morphologic analysis

Correspondence: Dra. Anna Merino *Department of Hemotherapy-Hemostasis,Core Laboratory, CDB, Hospital Clinic, Barcelona, Spain. amerino@clinic.ub.es*

2. Abstract

INTRODUCTION

The objective is to advance in the automatic, image-based, characterization and recognition of a heterogeneous set of lymphoid cells from peripheral blood, including normal, reactive and five groups of abnormal lymphocytes: hairy cells, mantle cells, follicular lymphoma, chronic lymphocytic leukemia and prolymphocytes.

METHODS

A number of 4,389 images from 105 patients were selected by pathologists, based on morphologic visual appearance, from patients whose diagnosis was confirmed by all the remaining complementary tests. Besides geometry, new color and texture features where extracted using six alternative color spaces to obtain rich information to characterize the cell groups. The recognition system was designed using support vector machines trained with the whole image set.

RESULTS

In the experimental tests, individual sets of images from 21 new patients were analyzed by the trained recognition system and compared with the true diagnosis. An overall recognition accuracy of 97.67% was achieved when the cell screening was done into three groups: normal lymphocytes, abnormal lymphoid cells and reactive lymphocytes. The accuracy of the whole experimental study was 91.23% when considering the further discrimination of the abnormal lymphoid cells into the specific five groups.

CONCLUSION

The excellent automatic screening of the three groups of normal, reactive and abnormal lymphocytes is useful since it discriminates between malignancy and not malignancy. The discrimination of the five groups of abnormal lymphoid cells is encouraging toward the idea that the system could be an automated image-based screening method to identify blood involvement by a variety of B lymphomas.

3. Main body of text

INTRODUCTION

The observation of the blood cells under the microscope provides very useful information and is the first analytical step in diagnosing most of the hematological diseases [1,2]. Lymphoid neoplasms or lymphomas may have a leukemic evolution in which abnormal cells circulate in peripheral blood (PB). Abnormal cell morphology, together with immunophenotype and genetic changes, remains essential to define lymphoid neoplasms [3]. Visual morphologic differentiation between subtypes of abnormal blood lymphoid cells requires much experience and skill. Objective measures do not exist to characterize cytological variables and some different B neoplastic lymphoma cells exhibit subtle differences in morphologic characteristics [4]. Lymphoid cells in follicular lymphoma (FL) and chronic lymphocytic leukemia (CLL) are often small, while mantle lymphoma cells are pleomorphic, varying in size and nucleus/cytoplasm ratio, showing a less condensation in chromatin with respect to CLL, and some cells may appear blastic with cleft nucleus and a prominent nucleolus [5]. Lymphoid cells in hairy cell leukemia (HCL) are larger than normal lymphocytes and have abundant pale blue-grey cytoplasm with fine hair-like projections. B-prolymphocytes (BPL) are twice the size of a normal lymphocyte and their nucleus has a central nucleolus and a chromatin moderately condensed. On the other hand, viral and other infectious processes also produce subtle morphological changes that may become confused with abnormal lymphoid cells.

The availability of quantitative descriptors of individual lymphoid cells may help to define morphologic features of malignant lymphocytes. It is possible to quantify cell morphology turning qualitative data into quantitative values by image analysis. Automatic methodologies for digital image processing of blood cells are able to pre-classify normal cells in different categories by applying neural networks, extracting a large number of measurements and parameters that describe the most significant cell morphologic characteristics [6-8]. Up to the author knowledge, the literature has reported classification tools able to recognize only a limited number of abnormal lymphoid cells [9-13].

The need for recognition of abnormal lymphocytes should not be underestimated, since some studies have demonstrated significant variability in their classification of abnormal lymphocytes [14]. In addition, lymphoid cell subtypes have been the most difficult to identify by the participants in hematology external quality assessment schemes [4]. Reactive lymphocytes, secondary to viral or bacterial infections, are a frequent finding in peripheral blood examination. It has been shown that the differentiation of reactive lymphocytes from abnormal neoplastic lymphoid cells may be difficult [14]. On the other hand, PB smear plays a critical role in the diagnosis and management of many lymphomas, since all the new high technology tests cannot be interpreted accurately without examining the peripheral blood film [15].

In previous studies [16,17], the basis of a method for lymphocyte recognition was presented for the automatic classification of four types of abnormal lymphoid cells circulating in PB in some mature B cell neoplasms: CLL, HCL, MCL and BPL.

The objective of this article is to extend the scope of the method with the inclusion of both reactive lymphocytes and follicular lymphoma cells. The introduction of two new groups of lymphoid cells implies more complexity in the automatic recognition, which requires methodological improvements in: (1) the introduction of new quantitative descriptors for a better discrimination of cells within a wider and more heterogeneous population; and (2) the development of an effective classification system able to accurately distinguish among subtypes of such heterogeneous population.

It is important to emphasize that an automatic recognition system is based on the pattern recognition paradigm. This involves methods and computer-based algorithms able to distinguish patterns within sets of data, which have to be consistent with human experience. In the development of such

systems, a "training" stage is required, in which significant amounts of data obtained in a wide variety of scenarios are needed because, once the system will be in operation in a "screening" stage, their results will be based on comparisons with respect to the trained patterns. In our case, data come from digital images containing a large number of pixels, which are described by numerical values corresponding to light intensity. The scenarios to recognize are the different cell image groups. In the training development, it is crucial to use a significant number of images of each type, arranging a big and heterogeneous set. Every time an existing system is aimed to augment with new cell groups, the training process has to be initiated from scratch with larger and varied number of descriptors and the final setup of a new recognition system.

Consequently, this article includes methodological advances in the cell characterization and recognition. Moreover, it describes a patient-based experimental evaluation: the input to the classification system is a set of digital cell images obtained from a PB blood smear of an individual patient selected for image analysis by the pathologist, based on the typical morphology of the disease group. The system output is the separation of the image set according to the different groups included in the study. The efficiency is analyzed focusing on two ways of screening:

1) The correct classification of the patient cell images in one of the following three big groups: normal, reactive or abnormal lymphocytes. This allows discern among malignancy and non-malignancy.
2) In case of malignancy, the correct recognition in one of the five abnormal lymphocytes considered in the system.

MATERIAL AND METHODS

This work is built from digital images of blood cells, which are analyzed through processes involving computational algorithms, which are finally combined in an input-output recognition system oriented towards a support tool for morphologic screening. This section describes the main

issues related to: (1) blood sample preparation, (2) image acquisition and processing, (3) feature extraction, 4) cell recognition, and (5) experimental testing of the recognition system.

Blood sample preparation

Samples from normal donors and patients with reactive lymphocytes, CLL, HCL, MCL and FL were used. Malignant diagnoses were confirmed by clinical and morphologic findings as well as immunophenotype of the lymphoid cells analyzed by flow cytometry and other complementary tests following the WHO classification of lymphoid neoplasms[3]. CLL cells had the phenotype CD5+, CD19+, CD23+, CD25+, weak CD20+, CD10-, FMC7- and dim surface immunoglobulin (sIg) expression. Atypical cases of CLL and the small proportion of lymphoid cells with cleaved nuclei were not included in our work. All HCL patients showed lymphoid cells with phenotype CD11c+, CD25+, FMC7+, CD103+ and CD123+. Patients with MCL had lymphoid cells with phenotype CD5+, FMC7+, CD43+, CD10- and BCL6-. In MCL cases, cyclin D1 was over-expressed and t(11;14) was found. Leukemic cells from follicular lymphoma were positive for the following B-cell associated antigens: CD19, CD20, CD22, CD79a, BCL2+, BCL6+, CD10+, CD5- and CD43-. B Prolymphocyte images were selected by their morphology (larger cells with nucleoli) in patients with CLL. Blood smears were obtained from the routine workload of the Core Laboratory of Hospital Clínic of Barcelona. Blood was collected into tubes containing K3EDTA as anticoagulant. Samples were analyzed by a cell counter Advia 2120 (Siemens Healthcare Diagnosis, Deerfield, USA) and PB films were automatically stained with May Grünwald-Giemsa in the SP1000i (Sysmex, Japan, Kobe) within 4 hours of blood collection.

Digital image acquisition and processing

All the individual lymphoid cell images were obtained using the CellaVision DM96 analyzer (Lund, Sweden), having a resolution of 363 x 360 pixels. After extraction, all further processes in this work were developed and implemented independently in a Dell Precision 5810 workstation with a Intel® Xeon® processor E5-1620 v3 " 3.50 GHz x 4, 16 GB RAM and a graphics card NVIDIA Quadro

K2200, by using the scientific software MATLAB®. Figure 1 shows a block diagram of these processes, being typical in any application involving digital image processing and machine learning algorithms [18,19]. For the developments, a training set was arranged with 4,389 lymphoid cell images, obtained from a total of 105 patients, and distributed as follows: 591 normal lymphocyte images from healthy patients (N), 423 RL, 512 HCL, 875 MCL, 561 FL and 1427 from patients with CLL. This group was divided into 1116 CLL clumped chromatin lymphocyte images and 311 BPL images. All these images were selected from PB films by the pathologists (AM and LB), based on their morphologic visual appearance typical of the disease entity, from patients in which the diagnosis was confirmed by all the remaining complementary tests [3].

Segmentation is a major step in digital image processing, where cells are separated from other objects in the image. In this work we used a previously developed algorithm [17], which was proven to be efficient to automatically separate the three regions of interest: nucleus, cell and peripheral zone around the cell. The cytoplasm was identified by the difference between the whole cell and the nucleus.

Feature extraction

From the segmented images, it is necessary to identify a set of quantitative descriptors that are relevant for the morphological analysis and the subsequent classification. Usually three types of descriptors are used: geometric, color and texture. Geometric descriptors are the most intuitive and closely related to the visual patterns that are familiar to pathologists. We extracted 13 parameters related to size and shape of both nucleus and cell [16], such as nucleus/cytoplasm ratio, nucleus perimeter, cytoplasmic profile and others.

Color is a physical property very common in the visual characterization of blood cells, and different spaces can be used for a quantitative representation. For instance, in RGB space, each color is decomposed in three bands corresponding to basic colors as red, green and blue. In this work, we

used six different color spaces [20]: RGB, CMYK, X*Y*Z, L*a*b*, L*u*v, and HSV. Our idea was to explore the rich amount of information that different types of components may offer about the different lymphoid cells, such as, for example, other colors like cyan, magenta and blue (from CMYK), or attributes like hue, saturation and brightness (in HSV), lightness (L) or chromaticity (a, b, u, v). For each region of interest of every segmented image, a histogram was calculated for each color space component. Histograms display the proportion of pixels on the image with specific intensity values. For each histogram, six classical first-order statistical features were calculated: mean, standard deviation, skewness, kurtosis, energy (uniformity) and entropy 1 (variability).

Texture refers to spatial patterns of color or intensities, which can be visually observed and quantitatively represented using statistical tools. To do this, the co-occurrence matrix is used, which defines the probability that pairs of neighbor pixels have similar intensities [21]. In practice, this probability is computed as the frequency of occurrences (second order histogram) divided by the number of neighbor pixels. In this work, histograms were obtained for each color space component, and then 17 second-order statistical descriptors [22] were calculated for each histogram.

In this study, texture was additionally characterized by using two more mathematical tools. One is the wavelet transform, which is widely used in image processing to analyze trends and fluctuations. The analysis of fluctuations in an image serves to characterize texture [23]. In this work, the wavelet transform was used for each cell image and then 12 statistical measures (means and standard deviations) were calculated as texture features. Granulometry approaches texture description by measuring the particle size distribution in an image by a series of operations within the mathematical morphology [24]. In this work eight granulometric features were calculated.

Finally, 43 features were defined for color and texture. When considering the six color spaces, we had 19 components, so that we had 817 features. Since we applied them separately to nucleus,

cytoplasm and the whole cell, a total of 2,451 color/texture features were obtained. All of them were determined for each image and stored in a numerical data set. Readers may find more technical details about those features and their calculations in [20].

Cell recognition

The objective of this step was to build a pattern recognition module (see Figure 1) composed by two elements: (1) a set of most relevant features selected among those extracted in the training stage; and (2) an algorithm (classifier) to perform the automatic identification among normal, reactive lymphocytes and the five B neoplastic lymphoid cell subsets. To face the significant number of lymphoid groups under study, several classification techniques were analyzed, the so-called support vector machine (SVM) with a radial basis function kernel [20, 25] being finally selected.

The overall classification accuracy and three more performance parameters were used for the classification evaluation: (1) sensitivity or true positive rate (TPR), (2) specificity or true negative rate (TNR), and (3) precision or positive predictive value (PPV).

Experimental recognition tests

After the selection of the best features and the tuning of the optimal classifier, a recognition system was assembled. The system input is a set of digital cell images obtained from a PB smear of an individual patient. The system output is the classification of this set into the different groups under study. To assess the system effectiveness, a number of 21 patients and sets of the corresponding images (946 in total) were selected by the pathologist (AM) based on their morphologic visual appearance. All the true diagnoses of the patients were confirmed by the corresponding complementary tests [3]. Images were obtained using the same smear staining and the same acquisition device as in the development stage, but they were not used before in the training. These are two important issues to remark, since pattern recognition, involving training and comparisons with reference characteristics, is the essential paradigm in building the recognition approach.

RESULTS

System development

As explained before, we obtained 2,464 features in the extraction step, 13 of them being geometric and the remaining color and texture features. Two issues were particularly important in deriving the classification system: (1) the selection of a reduced number of features, and (2) the tuning of the parameters of the SVM classifier [20, 25, 26]. Both issues are interconnected, as illustrated by the feedback arrow in Figure 1, since the quality of the selected features is measured by the accuracy in the classification. Iterative tests were performed where the classifier performance was evaluated using the 10-fold cross validation technique [17] over the whole image training set. At the end of this iterative tuning process, the best 150 features were ranked based on maximizing their relevance and minimizing their redundancy [28], and the classifier was finally designed and ready to be used in the further experimental study. Among these features, six were geometric (easily interpretable). The remaining 144 were color and texture features, which have an abstract interpretation in relation to the cell morphology.

To give some insight on these features, Table 1 lists the 15 most relevant, where nucleus-cytoplasm ratio (N/C), nucleus perimeter, cell diameter and cytoplasmic external profile (hairiness) are geometric. The remaining features are related to color and texture and we may observe that the six color spaces adopted in this work are involved. For instance, feature 4 is a statistical parameter describing the uniformity of the histogram of the hue component of the color space HSV. Feature 5 is related to texture (granulometry) and calculated from the XYZ space, while 6 is another texture feature calculated for the cyan component. It is worth to remark that some of the features in Table 1 were calculated from the nucleus, others from the cytoplasm and others from the whole cell.

Figure 2 shows box plots of features 1,2,4,5,6 and 11 calculated over the whole training set of 4,389

images separated for the seven cell groups. Each box contains the central 50% of the images in the group, and the line in the box represents the median. The length of the lines below and above represents the 25 and 75 quartiles. Some observations can be made in Figure 2 (a, b and f), which are consistent with the morphological characteristics of the different groups, such as the low N/C ratio in HCL and RL, the high heterogeneity of the MCL and the specific hairiness of HCL. A first insight on Figure 2 (c and d) shows that the two represented features (color/texture for the whole cell) exhibit similar patterns, HCL and RL being the groups with the lowest values. Figure 2 (e) represents a feature that exhibits a clear specificity for the CLL group. This granulometric feature is an abstract representation of texture, which has a difficult morphologic interpretation.

The classifier is a computerized algorithm designed with ability to relate a big number of features, building connections and leading to the recognition of a collection of cell groups. The performance of the final optimal classification of the 4,389 cell images included in the training set is highlighted by means of a confusion matrix in Table 2. Rows indicate the true diagnosis and columns represent the predicted diagnosis supplied by the classifier for each type of lymphoid cell. Every row is normalized in relation to the total number of cells of its respective type to obtain the percentages respect to the true diagnosis. Diagonal values are percentage numbers of the true positive rates for each cell subtype: 88.5% for normal lymphoid cells, 94.5% for HCL, 92.9% for CLL, 85.7% for FL, 89.1% for MCL, 83.0% for BPL and 94.1% for RL (see Table 2). The overall classification accuracy for the seven groups was 90.25%. The precision values were above 88.43% for all neoplastic lymphoid cell subtypes, normal and reactive lymphocytes. The sensitivity values were above 89.25% except for the normal cell subtype, in which sensitivity value was 100%. Finally, all the specificity values were above 98.09%.

Experimental recognition tests

The 21 patients for this study were selected in the following way: (a) 4 healthy individuals with

normal (N) lymphoid cells, (b) 5 patients with the diagnosis of infectious mononucleosis and having reactive lymphocytes (RL), and (c) 12 patients with B lymphoid cell neoplasms: HCL (3), MLC (2), FL (3) and CLL (4). For each individual, a variable number of images (minimum 10) were acquired as indicated in Table 3 (third column). Each set of images was processed by the recognition system independently of each other. An overall view of Table 3 highlights that the system was able to successfully recognize most of the cells corresponding to the true diagnosis, showing the following accuracy intervals for each subset: 100% for normal lymphocytes, [95%, 100%] for HCL cells, [70%, 96.9%] for FL cells, [77.5%, 98.2%] for CLL cells, [46%, 74%] for MCL cells, [68%, 97%] for BPL cells and [88.5%, 100%] for RL. The cell classification accuracy of the whole experimental study was 91.23%.

It is interesting to observe the data of Table 3 arranged in three groups: 1) normal lymphocytes (N), abnormal lymphoid cells (ALC) and reactive lymphocytes (RL). This is shown in Table 4. The diagonal values represent the true positive rates for each of the arranged groups: 100% for N, 97.9% for ALC and 95.7% for RL. The overall cell classification accuracy was 97.67%.

Figure 3 shows individual images from five patients of the experimental group. The first row shows lymphoid cell images (patient 7) that the system identified as HCL cells (32/32, 100%). The second row shows lymphoid cells that the system identified 63/65 (97%) as FL cells (patient 9, Table 3), diagnosis confirmed by complementary tests. A total of 55/71 of the cell images were classified as CLL cells (77%) and 8/71 were recognized as BPL in patient 12 and some of these images are shown in row 3. Fourth row corresponds to some of the 29/39 lymphoid cell images (74%) that were classified as MCL cells (patient 14). Finally, the fifth row corresponds to lymphoid cell images that were classified as reactive lymphocytes (patient 19). Most of the cell images corresponding to individual patients were automatically identified in the group corresponding to the true diagnosis

DISCUSSION

Recently, the International Council of Standardization in Hematology (ICSH) recommended using the term *reactive* to describe lymphocytes with morphological changes related to benign etiology and the term *abnormal* to describe lymphocytes with a suspected malignancy [5]. The morphologic discrimination among neoplastic B lymphomas is a significant added value that may be complementary to other additional tests, which cannot be interpreted accurately without examining the peripheral blood film [15]. However, these lymphoid cells are the most difficult to classify using only morphological features [4], and interpretation is based on individual experience. New techniques such as automated recognition systems are not able to differentiate the lymphocytes into reactive or abnormal [6-8, 28].

In this article, the goal of the recognition system was the automatic classification of normal, reactive and other lymphoid cells that were identified abnormal in 5 different neoplastic subsets of B lymphoma. This discussion is first focused on the results obtained by the recognition system when using separate sets of cell images from individual patients. In a first insight, we may observe Table 4 and conclude that the system was able to discriminate with excellent accuracy the three main groups: (1) normal lymphocytes, (2) reactive lymphocytes and (3) abnormal B lymphoma cells. This screening is highly valuable by itself, since it separates malignant from not malignant cells.

In a second insight, it is interesting to analyze the results given in Table 3 specifically for the five abnormal groups. It may be observed that, when using separate sets of cell images from individual patients, the system was able to successfully classify most of the cell images in the group corresponding to the true diagnosis. In the particular case of the recognition of FL and MCL lymphoid cells, some overlapping was found in patients 8 and 13. This can be understood due to the morphologic similarities existing between MCL cells and some FL cells [4,29]. Nevertheless, when both groups are considered together, the discrimination of such group from the others is excellent.

To obtain the satisfactory results presented in this paper, it was necessary to create a big knowledge base, with the extraction of a large and varied number of 2,464 features from many images corresponding to all the cell groups under study. Besides geometric/size characteristics, color and texture are attributes that play an essential role in the differential description of the lymphoid cell types [11]. Instead of working with only one color model, our strategy was to exploit the rich amount of information that six different color spaces may offer to describe the different lymphoid cells, what considerably increased the number of features. The availability of such rich information is the starting point for any pattern recognition problem. Many of these features may be irrelevant or redundant for the recognition, but this is not known a priori and is an advisable common practice to use any potentially useful information. The design of an efficient SVM classifier was done through iterative classification tests over the whole image training set, while progressively reducing the number of features. Computation is not a problem during the training, since this is part of an off-line development stage. However, the running time becomes important when analyzing patient smears in real time, so that the selection of the features and the design of the classifier has to involve a trade off between ensuring performance and reducing computational burden.

The final tuning process finished with the optimal selection of 150 meaningful features. The results in Table 2 display a satisfactory performance in terms of accuracy, sensitivity, specificity and precision. It is important to note that, within the most 15 relevant characteristics (Table 1 and Figure 2), several components of all the color spaces were involved, which indeed shows that the strategy of using a big number of color/texture features was satisfactory.

To our knowledge, the high number of lymphoid cell subtypes automatically recognized in this work has not been yet reported in the literature. A previous work [30] investigated the use of SVM classifiers to recognize five different types of normal leukocytes but only one subtype of abnormal lymphoid cells (CLL). In addition, a method was proposed [13] that was able to recognize five

types of blood cells, but the images selected were precursor lymphoid cells and myeloid blast cells from acute leukemia patients.

The need for recognition of abnormal lymphocytes should be recognized, since some studies have reported a significant variability in the classification of normal, reactive and abnormal lymphocytes. For instance, a survey using digital cell images [14] showed that 31% of the morphologists were not able to reproduce their own previous classification. New techniques, in particular automated recognition systems as the one presented in this article, may reduce the inter-observer variation and subjectivity of the classification.

As a feature work, other B and T abnormal cells should be characterized and included in the training and recognition scheme in view to have a general system able to classify any abnormal lymphocyte in a peripheral blood sample. Other subsets such as large granular lymphoid cells, plasma cells or neoplastic T cells should be also considered, as well as different lineages of blast cells.

The patient-based experimental tests included in this study have served to illustrate the potential capabilities of the proposed recognition method. A further step will be to define the minimum proportion of abnormal cells of each particular type detected by the recognition system necessary to accept the screening result as a guide toward the morphologic diagnosis. A wider number of patients covering the whole spectrum of pathologies will be required.

REFERENCES

1. Houwen B. The differential cell count. Lab Hematol 2001;7(2):89–100.

2. Bain BJ. Diagnosis from the blood smear. N Engl J Med 2005;353(5):498–507.

3. Swerdlow SH, Campo E, Harris NL, Jaffe ES, Pileri SA, Stein H, et al. WHO Classification of Tumours of Haematopoietic and Lymphoid Tissues. IARC Press; 2008.

4. Gutiérrez G, Merino A, Domingo A, Jou JM, Reverter JC. EQAS for peripheral blood morphology in Spain: a 6-year experience. Int J Lab Hematol 2008; 30(6): 460–6.

5. Palmer L, Briggs C, McFadden S, Zini G, Burthem J, Rozenberg G, et al. ICSH recommendations for the standardization of nomenclature and grading of peripheral blood cell morphological features. Int J Lab Hematol 2015; 37(3):287–303.

6. Ceelie H, Dinkelaar RB, van Gelder W. Examination of peripheral blood films using automated microscopy; evaluation of Diffmaster Octavia and Cellavision DM96. J Clin Pathol 2007; 60(1): 72–79.

7. Briggs C, Longair I, Slavik M, Thwaite K, Mills R, Thavaraja V, et al. Can automated blood film analysis replace the manual differential? An evaluation of the CellaVision DM96 automated image analysis system. Int J Lab Hematol 2009; 31(1): 48–60.

8. Briggs C, Culp N, Davis B, D'Onofrio G, Zini G, Machin SJ. ICSH guidelines for the evaluation of blood cell analysers including those used for differential leucocyte and reticulocyte counting. Int J Lab Hematol 2014; 36: 613-627.

9. Foran DJ, Comaniciu D, Meer P, Goodell LA. Computer-assisted discrimination among malignant lymphomas and leukemia using immunophenotyping, intelligent image repositories and telemicroscopy. IEEE Trans Inf Technol Biomed 2000; 4(4): 265–73.

10. Sabino DMU, Dafontouracosta L, Gilrizzatti E, Antoniozago M, da Fontoura Costa L, Gil Rizzatti E, et al. A texture approach to leukocyte recognition. Real-Time Imaging 2004; 10(4): 205–16.

11. Angulo J, Klossa J, Flandrin G. Ontology-based lymphocyte population description using mathematical morphology on colour blood images. Cell Mol Biol 2006; 52(6): 2–15.

12. Tuzel O, Yang L, Meer P, Foran DJ. Classification of hematologic malignancies using texton signatures. Pattern Anal Appl PAA 2007; 10(4): 277–90.

13. Yang L, Tuzel O, Chen W, Meer P, Salaru G, Goodell L a., et al. PathMiner: a Web-based tool for computer-assisted diagnostics in pathology. IEEE Trans Inf Technol Biomed 2009; 13(3): 291–9.

14. van der Meer W, van Gelder W, de Keijzer R, Willems H. The divergent morphological classification of variant lymphocytes in blood smears. J Clin Pathol 2007; 60(7): 838–9.

15. Hernández AM. Peripheral blood manifestations of lymphoma and solid tumors. Clin. Lab. Med.2002; 22(1): 215–52.

16. Alférez S, Merino A, Mujica LE, Ruiz M, Bigorra L, Rodellar J. Automatic classification of atypical lymphoid B cells using digital blood image processing. Int J Lab Hematol 2014; 36(4): 472–80.

17. Alférez S, Merino A, Bigorra L, Mujica L, Ruiz M, Rodellar J. Automatic recognition of atypical lymphoid cells from peripheral blood by digital image analysis. Am J Clin Pathol 2015; 143:168–76.

18. Gonzalez RC, Woods RE. Digital Image Processing (3rd Edition). 3rd ed. Prentice Hall; 2007.

19. Bishop CM. Pattern recognition and machine learning. springer; 2006.

20. Alférez S. Methodology for Automatic Classification of Atypical Lymphoid Cells from Peripheral Blood Cell Images. Doctoral Thesis, Universitat Politècnica de Catalunya, Barcelona, Spain, 2015.

21. Haralick RM, Shanmugam K, Dinstein I. Textural features for image classification. IEEE Trans Syst Man Cybern 1973; 3(6):610–21.

22. Albregtsen F. Statistical Texture Measures Computed from Gray Level Coocurrence Matrices. Image Processing Laboratory, Department of Informatics, University of Oslo; 1995.

23. Arivazhagan S, Ganesan L. Texture classification using wavelet transform. Pattern Recognit Lett 2003; 24(9-10):1513–21.

24. Angulo J. A mathematical morphology approach to cell shape analysis. In: Bonilla LL, Moscoso M, Platero G, Vega JM (eds). Progress in Industrial Mathematics at ECMI 2006. Berlin, Heidelberg: Springer; 2008:2–6.

25. Steinwart I, Christmann A. Support Vector Machines. Springer; 2008.

26. Chang C-C, Lin C-J. LIBSVM. ACM Trans Intell Syst Technol 2011;2(3):1–27.

27. Brown G, Pocock A, Zhao M-J, Luján M. Conditional likelihood maximization: a unifying framework for information theoretic feature selection. J Mach Learn Res 2012; 13(1):27–66.

28. Merino A, Brugués R, García R, Kinder M, Torres F, Escolar G. Estudio comparativo de la morfología de sangre periférica analizada mediante el microscopio y el CellaVision DM96 en enfermedades hematológicas y no hematológicas (in Spanish). Rev del Lab Clínico 2011; 4(1):3–14.

29. Merino A. Manual de Citología de Sangre Periférica (in Spanish). Grupo Acción Médica; 2005.

30. Ushizima DM, Lorena AC, de Carvalho ACPLF. Support vector machines applied to white blood cell recognition. In: Fifth International Conference on Hybrid Intelligent Systems (HIS'05). IEEE; 2005:6.

Tables and Figures caption List

Table 1. The 15 most relevant features selected (from 150) based on maximizing the relevance and minimizing the redundancy. STD: standard deviation.

Table 2: Classification results (confusion matrix) for the training set of peripheral blood lymphoid cell images. The rows represent the true diagnosis and the columns the predicted diagnosis given by the classifier for each type of lymphoid cell. The values are in percentage. Diagonal values are the true positive rates for each cell subtype. Global accuracy = 90.25%.

Table 3: Classification results obtained in the experimental testing of the recognition system. For each single patient, a number of images were acquired (third column) and classified into the seven different groups. Global cell classification accuracy = 91.23%.

Table 4. Results of Table 3 arranged in three groups: normal lymphocytes (N), reactive lymphocytes (RL) and abnormal lymphoid cells (ALC). The rows represent the true diagnosis and the columns the predicted diagnosis. The diagonal values represent the global accuracy for each group. The values are in percentage with respect to the total number of each (true) type of cell.

Figure 1. Block diagram illustrating the steps followed to develop the recognition system. A training set of lymphoid cell images are processed, including segmentation, to obtain a database of features. A recognition module is built which includes a classifier based on support vector machines (SVM), whose input is a reduced number of most relevant features. The final selection of the best features and the tuning of the best classifier are performed jointly through an iterative process, involving 10-cross validation, where the quality of the features is determined by the efficiency of the classifier.

Figure 2. Box plots of relevant features 1(a), 2(b), 4(c), 5(d), 6(e) and 11(f), from Table 1, calculated over the whole training set of 4,389 images for the seven cell groups included in this work. Each box contains the central 50% of the images in the group, and the line in the box represents the median. The length of the lines below and above represents the 25 and 75 quartiles.

Figure 3. Five cases analyzed with the recognition system. Each row shows examples of atypical lymphoid cell images from a single patient, which have been correctly classified in one of the groups under study. Magnifications: *x*1000. Stain: MGG. Note also the excellent segmentation of the three regions of interest: nucleus, cell and peripheral zone.

Table 1. The 15 most relevant features selected (from 150) based on maximizing the relevance and minimizing the redundancy. STD: standard deviation.

1	Nucleus – cytoplasm ratio
2	Nucleus perimeter
3	Cell diameter
4	Cell energy of the histogram of the Hue (HSV)
5	STD of the Pseudo-granulometric curve of the X component (XYZ) of the cell
6	Information measure of correlation 1 of the Cyan (CMYK) of the nucleus
7	Kurtosis of the v component (L*u*v*) of the cell
8	Kurtosis of the Saturation (HSV) of the cell
9	STD of the red (RGB) of the cell
10	Mean of the b component (L*a*b*) of the nucleus
11	External profile feature
12	Correlation of the Cyan (CMYK) of the nucleus
13	Kurtosis of the Pseudo-granulometric curve of the Cyan (CMYK) of the cell
14	Mean of the Pseudo-granulometric curve of the Cyan (CMYK) of the nucleus
15	STD of the Pseudo-granulometric curve of the Blue (RGB) of the cytoplasm

Table 2: Classification results (confusion matrix) for the training set of peripheral blood lymphoid cell images. The rows represent the true diagnosis and the columns the predicted diagnosis given by the classifier for each type of lymphoid cell. The values are in percentage. Diagonal values are the true positive rates for each cell subtype. Global accuracy = 90.25%.

		Predicted						
		N	**HCL**	**FL**	**CLL**	**MCL**	**BPL**	**RL**
	N	**88.5**	1.0	0.8	6.3	0.8	1.4	1.2
	HCL	1.6	**94.5**	0.0	0.4	0.6	0.2	2.7
	FL	1.2	0.2	**85.7**	3.0	8.2	1.2	0.4
True	**CLL**	3.9	0.2	1.3	**92.9**	0.9	0.6	0.2
	MCL	0.5	0.1	6.4	1.6	**89.1**	1.5	0.8
	BPL	2.3	1.0	1.0	2.9	5.8	**83.0**	4.2
	RL	1.2	2.4	0.0	0.0	0.7	1.7	**94.1**

N, normal lymphocytes; HCL, hairy cell leukemia; CLL, chronic lymphocytic leukemia; FL, follicular lymphoma; MCL, mantle cell leukemia; BPL, B-prolymphocytes; RL, reactive lymphocytes.

Table 3: Classification results obtained in the experimental testing of the recognition system. For each single patient, a number of images were acquired (third column) and classified into the seven different groups. Global cell classification accuracy = 91.23%.

Patient	True diagnosis	Cell images	Accuracy	N	HCL	FL	CLL	MCL	BPL	RL
1	N	16	100.0	**16**	0	0	0	0	0	0
2	N	14	100.0	**14**	0	0	0	0	0	0
3	N	11	100.0	**11**	0	0	0	0	0	0
4	N	15	100.0	**15**	0	0	0	0	0	0
5	HCL	20	95.0	1	**19**	0	0	0	0	0
6	HCL	52	100.0	0	**52**	0	0	0	0	0
7	HCL	32	100.0	0	**32**	0	0	0	0	0
8	FL	81	70.4	0	0	**57**	1	23	0	0
9	FL	65	96.9	0	0	**63**	0	2	0	0
10	FL	73	93.2	1	0	**68**	2	2	0	0
11	CLL	165	98.2	1	0	2	**162**	0	0	0
12	CLL	71	77.5	4	1	2	**55**	1	8	0
13	MCL	13	46.2	1	0	5	1	**6**	0	0
14	MCL	39	74.4	0	0	1	0	**29**	7	2
15	BPL	64	95.3	1	0	0	0	2	**61**	0
16	BPL	53	90.6	3	0	0	0	1	**48**	1
17	RL	10	100.0	0	0	0	0	0	0	**10**
18	RL	53	98.1	0	1	0	0	0	0	**52**
19	RL	29	100.0	0	0	0	0	0	0	**29**
20	RL	26	88.5	0	0	2	0	0	1	**23**
21	RL	44	93.2	0	1	1	0	0	1	**41**

HCL, hairy cell leukemia; MCL, mantle cell leukemia; FL, follicular lymphoma; CLL, chronic lymphocytic leukemia; BPL, B-prolymphocytes; N, normal lymphocytes; RL, reactive lymphocytes.

Table 4. Results of Table 3 arranged in three groups: normal lymphocytes (N), reactive lymphocytes (RL) and abnormal lymphoid cells (ALC). The rows represent the true diagnosis and the columns the predicted diagnosis. The diagonal values represent the global accuracy for each group. The values are in percentage with respect to the total number of each (true) type of cell.

		Predicted		
		N	**ALC**	**RL**
	N	**100**	0	0
True	**ALC**	1.7	**97.9**	0.4
	RL	0	4.3	**95.7**

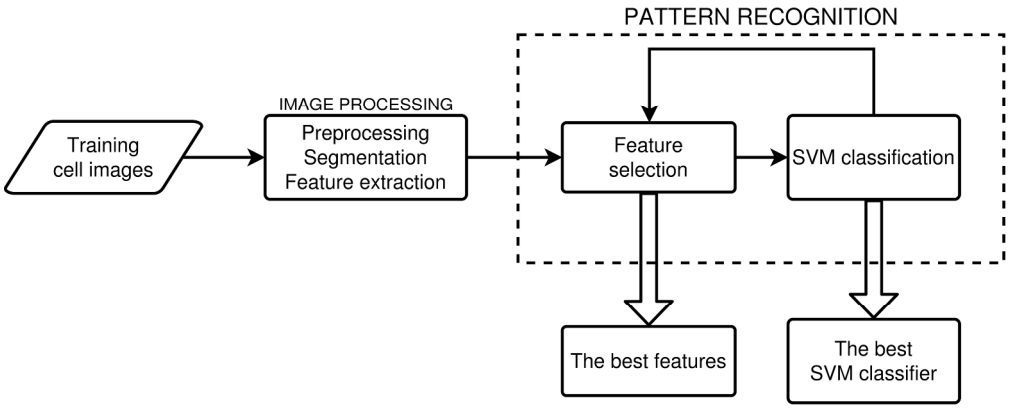

235x93mm (300 x 300 DPI)

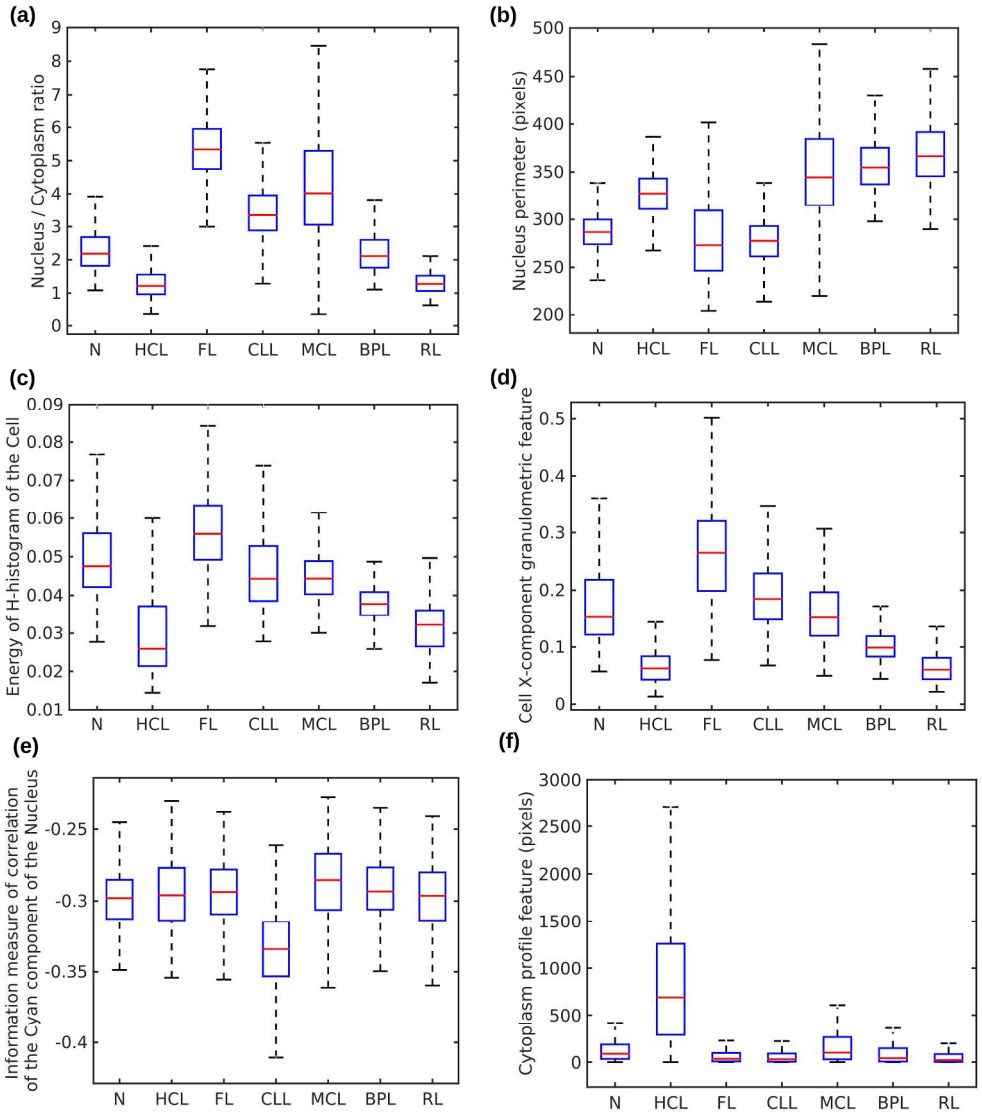

238x267mm (300 x 300 DPI)

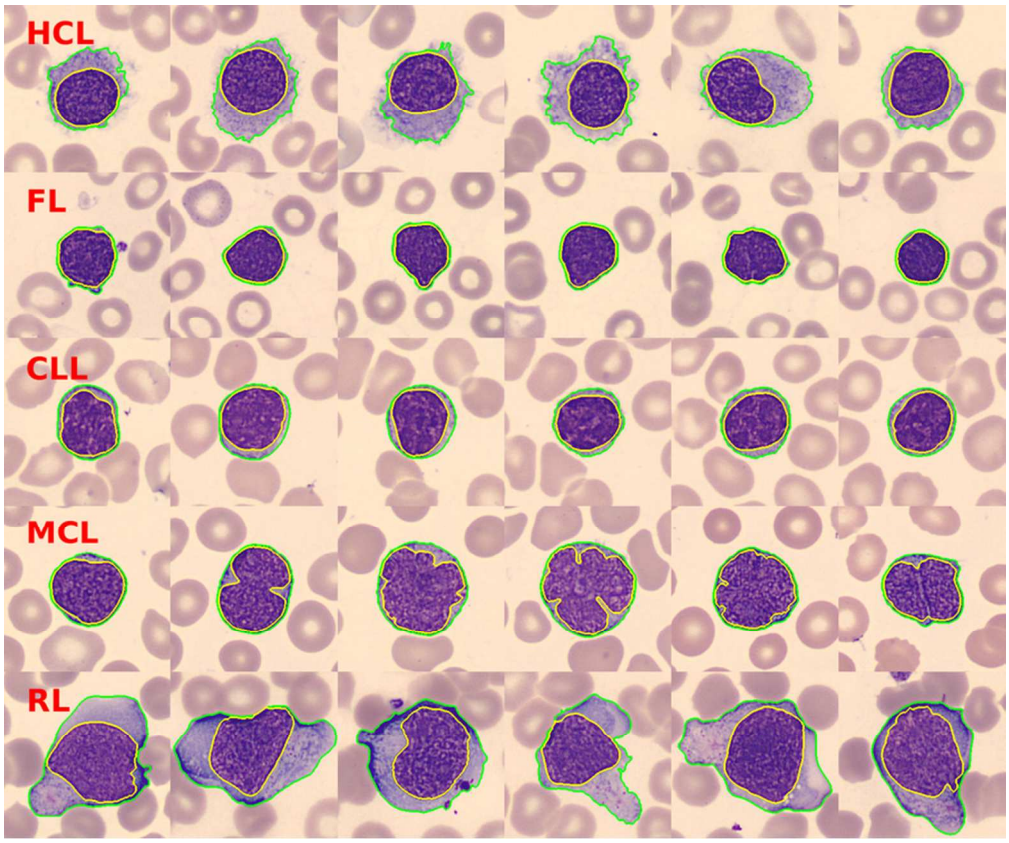

76x63mm (300 x 300 DPI)